

Article

# Multivariable PID Decoupling Control Method of Electroslag Remelting Process Based on Improved Particle Swarm Optimization (PSO) Algorithm

Jie-Sheng Wang \*, Chen-Xu Ning and Yang Yang

School of Electronic and Information Engineering, University of Science and Technology Liaoning, Anshan 114044, Liaoning, China; E-Mails: NCX710754167@163.com (C.-X.N.); wudianyiban@163.com (Y.Y.)

\* Author to whom correspondence should be addressed; E-Mails: wang\_jiesheng@126.com; wangjiesheng@ustl.edu.cn.

Received: 11 January 2014; in revised form: 1 February 2014 / Accepted: 7 February 2014 / Published: 18 February 2014

---

**Abstract:** A mathematical model of electroslag remelting (ESR) process is established based on its technical features and dynamic characteristics. A new multivariable self-tuning proportional-integral-derivative (PID) controller tuned optimally by an improved particle swarm optimization (IPSO) algorithm is proposed to control the two-input/two-output (TITO) ESR process. An adaptive chaotic migration mutation operator is used to tackle the particles trapped in the clustering field in order to enhance the diversity of the particles in the population, prevent premature convergence and improve the search efficiency of PSO algorithm. The simulation results show the feasibility and effectiveness of the proposed control method. The new method can overcome dynamic working conditions and coupling features of the system in a wide range, and it has strong robustness and adaptability.

**Keywords:** electroslag remelting process; multivariable system; PID controller; particle swarm optimization algorithm

---

## 1. Introduction

The electroslag remelting (ESR) process is an advanced smelting method to make purified steels based on rudiment steel in order to reduce impurity and get the high-quality steel which is defined by: uniformity, density and crystal in vertical [1]. The main purpose of the ESR process is to purify metal

and get the ingot with uniform density crystallization. The steel undergoing the ESR process has many advantages, such as high-purity, lower sulfur and inclusion of nonmetal, smooth surface of the ingot, the uniform density crystallization and the uniform metal structure and chemical composition [2,3].

From the control point of view, the ESR process is a typical complex controlled object, which has multi-variable, distributed parameters, nonlinear and strong coupling features. During the early stage of research, the normal control methods include voltage swings, constant current, constant voltage and descending power. The voltage swing control method is adopted to adjust the voltage swing amplitude in order to control the electrode movements and maintain the stability of slag resistance [4]. The reference [5] mainly discusses the key technology of melting speed control. The mathematical model of the time-variant system does not analyse the fundamental reasons causing voltage fluctuation at the expense of the current control accuracy in exchange for the smoothly control of the voltage swing. With the development of the control theory and modern optimization algorithm, the intelligent control strategies, which do not strictly depend on a mathematical model, are used in the ESR process. The reference [6] analyzes the ESR model, adopts the cooperative control method for the melting rate and position of remelting electrodes, whose parameters are optimized by the improved genetic algorithm. The reference [7] proposes an intelligent control method for the ESR process, which combines a variable frequency drive control strategy with the artificial neural network theory. The experimental results show that the proposed control strategy improves the accuracy and intelligence level of the ESR furnace, stables the remelting current.

The proportional-integral-derivative (PID) controller is widely used in many industrial processes because it is simple in structure, and has good robustness and high reliability. The self-tuning and optimization of the PID controller parameters is a very important research field [8,9]. With the rapid development of swarm intelligent theory, many PID controller parameters self-tuning methods based on the swarm intelligent theory appeared, such as genetic algorithm (GA), particle swarm algorithm (PSO), *etc.* [10–14]. Genetic algorithm adopts the duplication, crossover and mutation operators, whose performance has a larger dependence on parameters. On the other hand, PSO will easily lead to the local optima and produce early-maturation phenomena. According to dynamic characteristics of the ESR process, this paper establishes the mathematical model of the ESR process, and puts forward a kind of multivariable self-setting PID control strategy based on improved particle swarm optimization algorithm. The simulation results indicate that the proposed control method is feasible and effective.

The paper is organized as follows. In Section 2, the technique flowchart and mathematics model of the ESR process are introduced. In Section 3, the self-tuning of multivariable PID controller parameters based on IPSO is summarized. In Section 4, experiment and simulation results are introduced in details. Finally, the conclusion constitutes the last part.

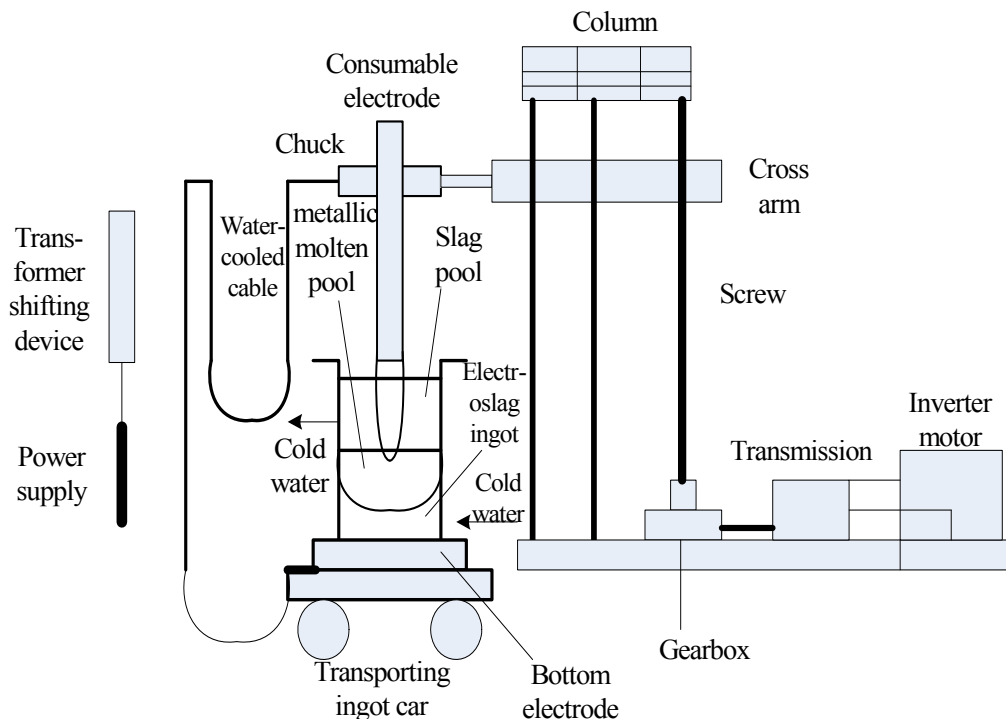
## **2. Technique Flowchart and Mathematics Model of ESR Process**

### *2.1. Technique Flowchart*

Electroslag furnace is a complex controlled object, whose production technique is more complex than other steelmaking methods [15,16]. There is still no good mathematical model to describe the ESR process. In order to ensure the stability of the ESR process and quality of the remelting metal, the

reasonable technique parameters must be chosen. The technique flowchart of electroslag furnace is described in the Figure 1.

**Figure 1.** Technique flowchart of the ESR furnace.



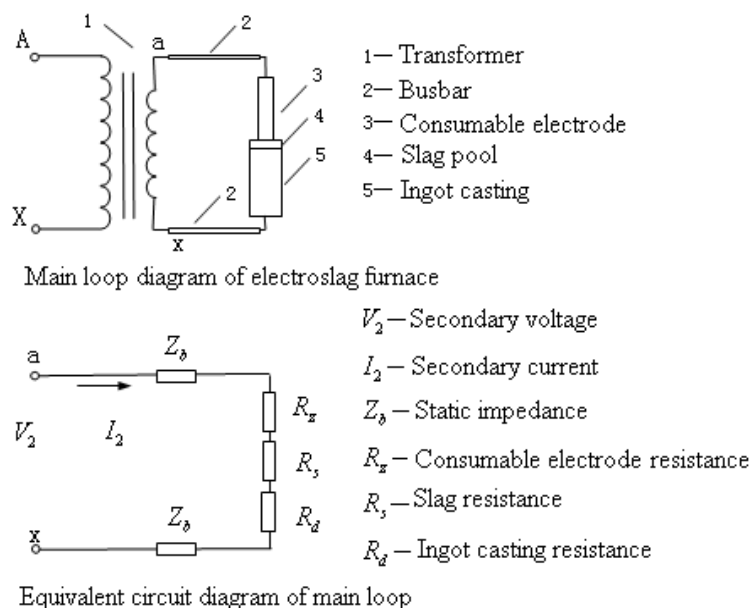
The operation flow of the ESR process is illustrated as follows: Add slag→Start arc→Melting slag→Casting→Feeding→Remelting end→Thermal insulation→Finished product. The technique of electroslag furnace may be divided into four stages: melting slag stage, exchange electrodes stage, casting stage and feeding stage.

- (1) Melting slag stage. It includes an opening stage to make slag and slag melting with low power by using the lower voltage and current. Because the slag pool has not been formed, there will be large current fluctuations. When the slag pool is formed, the current becomes stable. The slag will be melted until all slag materials have been added. From now on, slag melting will be put under a high power to melt all slag and keep a certain temperature.
- (2) Exchange electrodes. They will be finished by the movement of the robot arm, which should be finished in no more than five minutes to avoid the solidification of the melted electroslag. After the completion of the electrode exchange, because there will large heat absorption after the cold metal electrodes are inserted into the electroslag pool, the normal casting should not begin. To achieve the melting speed required by the steel casting technique, the current set-point must be increased.
- (3) Casting stage. The electrode melting velocity in the normal casting stage is the key factor of deciding the solidification of steel ingot. So the biggest allowed electrode melting velocity of the electroslag furnace may be concluded in accord with the related formulas.
- (4) Feeding stage. The main function of the feeding stage is to remove the pit on the top of the ingot caused by the solidification.

2.2. Mathematic Model

The main circuit of the electroslag furnace consists of a power supply whose voltage and current can be adjusted, a consumable electrode, electroslag, crystallizer, ingot casting and bilge chest. The major loop and its equivalent circuit are shown in the Figure 2.

Figure 2. Main circuit and equivalent circuit of ESR process.



The relationship between the voltage and current of electroslag furnace’s major loop is described as follows [1]:

$$V_2(t) = I_2(t) \times \left[ R_s + R_v + jX_l + K_1 (r^2 - 1) \cdot \int_{t_0}^t v(t) dt \right] \tag{1}$$

where  $V_2(t)$  is secondary voltage,  $I_2(t)$  is smelting current,  $R_s$  is slag resistance,  $R_v + jX_l$  is short impedance,  $r$  is filling ratio,  $v(t)$  is melting velocity and  $K_1$  is the resistance coefficient of steel grades.

The melting velocity of the electroslag furnace is mainly decided by the voltage and current. Its relationship is described as follows:

$$v(t) = K_2 I_2(t)^2 \cdot R_s \tag{2}$$

where  $K_2$  is the coefficient of melting velocity. Without taking into account the influences of the environment temperature and the cooling water, if the melting velocity is kept constant under the constant slag resistance, the control given model for melting current are defined as:

$$I_2(t) = \frac{K_3}{(1+t)^2} + K_4 \tag{3}$$

where  $K_3$  and  $K_4$  are the initial current coefficient and current equilibrium coefficient. In order to keep outlet voltage stable, the secondary voltage should be calculated by the following formula:

$$V_2(t) = \frac{K_5}{(1+t)^2} + K_6 - K_7(1-r^2)t \tag{4}$$

where  $K_5$  is initial voltage coefficient,  $K_6$  is current equilibrium coefficient and  $K_7$  is the changeable ratio coefficient of the consumable electrode and ingot resistance.

On the premise of the controlled object under steady working conditions, the system transfer functional is decided by the step response. By imposing the step disturbance to the secondary voltage  $V_2$  and the melting current  $I_2$  respectively, the step response curve of the excitation voltage  $\Delta V$  and the melting velocity  $v$  are calculated. On the basis of considering the variable dimension, the transfer function matrix of the electroslag furnace under the given working conditions obtained by the curve fitting method is illustrated as follows:

$$\begin{bmatrix} \Delta V(s) \\ v(s) \end{bmatrix} = \begin{bmatrix} G_{11}(s) & G_{12}(s) \\ G_{21}(s) & G_{22}(s) \end{bmatrix} \begin{bmatrix} V_2(s) \\ I_2(s) \end{bmatrix} = \begin{bmatrix} \frac{2.7s + 5.4}{3s^2 + 15s + 18} & \frac{0.33s^3 + 1.65s^2 + 2.31}{s^3 + 5s^2 + 18s} \\ \frac{8.1s + 16.2}{s^2 + 4s + 7} & \frac{s^2 + 8s + 7}{s^3 + 4s^2 + 7s} \end{bmatrix} \begin{bmatrix} V_2(s) \\ I_2(s) \end{bmatrix} \quad (5)$$

### 3. Self-Tuning of Multivariable PID Controller Parameters Based on IPSO

#### 3.1. Multivariable PID Control Strategy

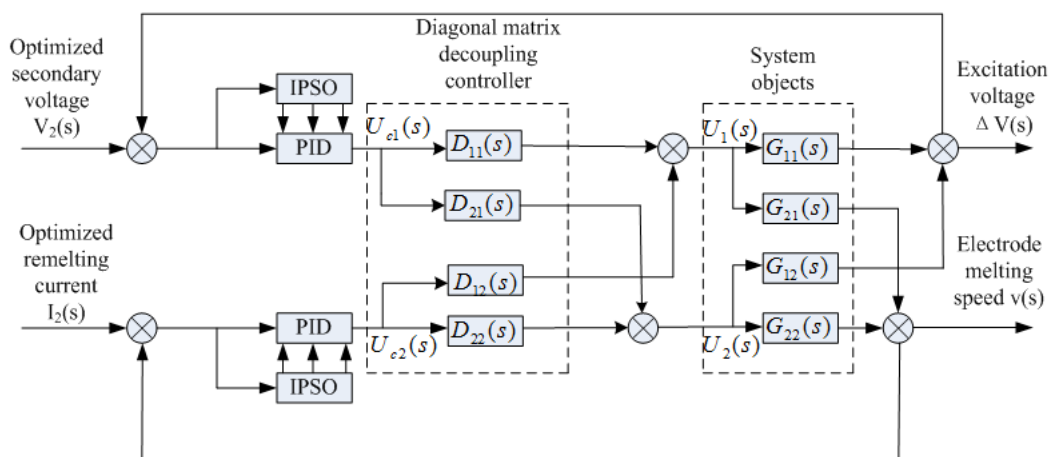
The PID controller is a regulator in accordance with the linear combination of the proportion, differential and integral of the error, which can be described as:

$$u(t) = K_p \left[ e(t) + \frac{1}{T_i} \int_0^t e(t) dt + \frac{T_d}{dt} de(t) \right] \quad (6)$$

where  $K_i = K_p / T_i$ ,  $K_d = K_p T_d$ , and  $e(t)$  is the feedback error.

According to the dynamic characteristics of ESR process, the paper puts forward a self-tuning multivariable PID control strategy optimized by the IPSO, whose structure is shown in Figure 3. The system is formed by the PID controller, the diagonal matrix decoupling module and the controlled object. The structure of ESR process multi-variable PID controller which this paper proposed is shown in Figure 3. It uses diagonal matrix decoupling control to eliminate the coupling of the original coupling system between each channel, and improve particle swarm algorithm to optimize control parameters of PID controller.

**Figure 3.** Configuration of self-tuning PID decoupling control system.



### 3.2. Diagonal Matrix Decoupling

According the above discussion, the system model can be represented as:

$$[x]_{ind(P)} = \bigcap_{R \in P} [x]_R \tag{7}$$

In order to realize the decoupling control of ESR process, the diagonal matrix decoupling method is adopted, which is described as follows:

$$G_{11}(s)D_{12}(s) + G_{12}(s)D_{22}(s) = 0 \tag{8}$$

$$G_{21}(s)D_{11}(s) + G_{22}(s)D_{21}(s) = 0 \tag{9}$$

Thus, Equations (10) and (11) are obtained based on the transfer functions of the controlled object and the diagonal matrix decoupling strategy.

$$\frac{D_{12}(s)}{D_{22}(s)} = -\frac{G_{12}(s)}{G_{11}(s)} = -\frac{0.33s^3 + 1.65s^2 + 2.31}{s^3 + 5s^2 + 18s} \bigg/ \frac{2.7s + 5.4}{3s^2 + 15s + 18} \tag{10}$$

$$\frac{D_{11}(s)}{D_{21}(s)} = -\frac{G_{22}(s)}{G_{21}(s)} = -\frac{s^2 + 8s + 7}{s^3 + 4s^2 + 7s} \bigg/ \frac{8.1s + 16.2}{s^2 + 4s + 7} \tag{11}$$

Finally, the transfer functions after decoupling disposal of ESR process are calculated as follows:

$$G_{11}^*(s) = \frac{2.7s + 5.4}{3s^2 + 15s + 18} \tag{12}$$

$$G_{22}^*(s) = \frac{s^2 + 8s + 7}{s^2 + 15s + 18} \tag{13}$$

So the system transfer function matrix after decoupling can be expressed as:

$$\begin{bmatrix} \Delta V(s) \\ v(s) \end{bmatrix} = \begin{bmatrix} G_{11}^*(s) & 0 \\ 0 & G_{22}^*(s) \end{bmatrix} \begin{bmatrix} V_2(s) \\ I_2(s) \end{bmatrix} \tag{14}$$

After decoupling, the original coupling system is decomposed into two independent, insusceptible single-input/single-output (SISO) control channels (System 1 and System 2) shown in Equations (15) and (16).

$$\Delta V(s) = G_{11}^*(s)V_2(s) \tag{15}$$

$$v(s) = G_{22}^*(s)I_2(s) \tag{16}$$

The hybrid PSO algorithm is utilized to optimize the parameters of two PID controllers in order to obtain the better control performances. The design of the PID controller is actually a multidimensional function optimization problem in essence, so the improved PSO algorithm adopts real value coding pattern. The multi-variable PID controller of ESR process can be directly coded as follows.

$$X = \left\{ \underbrace{K_{p1}, K_{i1}, K_{d1}}_{PID_1}, \underbrace{K_{p2}, K_{i2}, K_{d2}}_{PID_2} \right\} \tag{17}$$

The optimization object of the PID Controller parameters is to make the system overall control deviation tend to zero, and have a fast response speed and smaller overshoot. So the four error integral criterions described as follows are used to evaluate the control effect.

(1) Integral of squared error (ISE)

$$ISE = \int_0^{\infty} e(t)^2 dt \quad (18)$$

(2) Integral of time squared error (ITSE)

$$ITSE = \int_0^{\infty} t^2 e(t)^2 dt \quad (19)$$

(3) Integral of absolute error (IAE)

$$IAE = \int_0^{\infty} |e(t)| dt \quad (20)$$

(4) Integral of time multiplied by absolute error (ITAE)

$$ITAE = \int_0^{\infty} t |e(t)| dt \quad (21)$$

### 3.3. Particle Swarm Optimization Algorithm

Particle swarm optimization algorithm [17–19] is a kind of swarm intelligence evolution computing technology originating from the flock foraging behavior. Usually, a particle swarm is composed of  $M$  particles and the position of these particles  $X_i$  ( $i = 1, 2, \dots, M$ ) stands for the potential solutions in the  $D$  dimension. The possibility of the potential better solution is larger in the neighborhood space of good particles. These particles fly with a speed  $V_i$  according to the flight experiences of the individuals and groups, which is adjusted dynamically in  $D$  search space. The best position which each particle experiences indicates  $pbest$  [ $i$ ], and the best particle position in the whole swarm indicates  $gbest$  [ $g$ ]. The velocity and position of the particles are adjusted according to the following formula.

$$V_i = V_i + c_1 \cdot Rand() \cdot (pbest[i] - X_i) + c_2 \cdot rand() \cdot (gbest[g] - X_i) \quad (22)$$

$$X_i = X_i + V_i \quad (23)$$

where  $c_1$  and  $c_2$  are given constants called learning factors, and  $rand()$  is a random number within range  $[0, 1]$ .

In the course of the evolution of the flight speed  $V_i$ , the inertia weight  $w$  is introduced to increase the particle's motion inertia, expand the search space and improve the convergence of the discussed PSO algorithm. The PSO algorithm with inertia weights is described as follows:

$$V_i = w \cdot V_i + c_1 \cdot Rand() \cdot (pbest[i] - X_i) + c_2 \cdot rand() \cdot (gbest[g] - X_i) \quad (24)$$

### 3.4. Adaptive Chaotic Migration Mutation Operator

The genetic distance in GA is introduced to PSO algorithm, in which the particles diversity in the particle swarm is determined by the particle genetic distance. On the basis of this, a special mutation

operation (adaptive chaotic migration mutation operator) is utilized to process the particles sinking into gathered area [20,21].

When the position of the particle  $i$  is  $X_{id}(t)$  in the  $t$  generation and the global optimal value of particle swarm is  $P_{gd}(t)$ , the particle genetic distance relative to the  $P_{gd}(t)$  is defined as follows:

$$\sigma_i(t) = \sqrt{\frac{1}{D} \sum_{d=1}^D \left( \frac{X_{id}(t) - P_{gd}(t)}{2} \right)^2} \tag{25}$$

$$\bar{\sigma}(t) = \frac{1}{N_{pop}} \sum_{i=1}^{N_{pop}} \sigma_i(t) \tag{26}$$

where  $\sigma_i(t)$  is the genetic distance of particle  $i$  relative to the overall swarm,  $\bar{\sigma}(t)$  is the population mean genetic distance and  $N_{pop}$  is population size.

All particles, whose genetic distance is less than the average genetic distance, consist of a new particle group  $S_{opt}$ , in which the average distance of particles in new swarm is defined as  $\bar{\sigma}_{opt}(t)$ :

$$\bar{\sigma}_{opt} = \frac{1}{|S_{opt}|} \sum_{i=1}^{|S_{opt}|} \sigma_i(t) \tag{27}$$

where  $|S_{opt}|$  is the particle number in particle swarm  $S_{opt}$ . The smaller  $\bar{\sigma}_{opt}(t)$ , the higher the degree of particle collection. Set the valve value of collection degree  $\sigma^*$ , when  $\bar{\sigma}_{opt}(t) \leq \sigma^*$ , the particle swarm  $|S_{opt}|$  is carried out the mutation operation to enhance the diversity of the particle swarm.

Before the mutation operation, the particle swarm  $S_{opt}$  need to be carried out the chaos optimization. According to the Logistic mapping principle, a chaos optimization system is realized based on the following equation:

$$z_{k+1} = \mu \cdot z_k (1 - z_k) \tag{28}$$

where  $z_k$  is the number sequence within the scope of (0,1) and  $\mu$  is the number sequence within the scope of [3.571448,4].

Suppose the disturbance quantity of a chaotic system is  $\Delta x = (\Delta x_1, \Delta x_2, \dots, \Delta x_n)$  and the disturbance range is  $[-\beta, \beta]$ . Each component of  $z_k$  is carried to the disturbance range:

$$x_{id}(t+1) = x_{id}(t) + v_{id}(t+1) + \Delta x \tag{29}$$

The former  $|S_{opt}|$  with minimum fitness replaces the original particle swarm  $S_{opt}$ . Then the migration mutation operation is carried out based on the following rules.

$$x_{id}(t+1) = \lambda \cdot x_{id}^{(3)}(t) + (1-\lambda) \cdot P_{gd}(t) + F \cdot (x_{id}^{(1)}(t) - x_{id}^{(2)}(t)) \tag{30}$$

$$\lambda = \frac{T-t}{T} \tag{31}$$

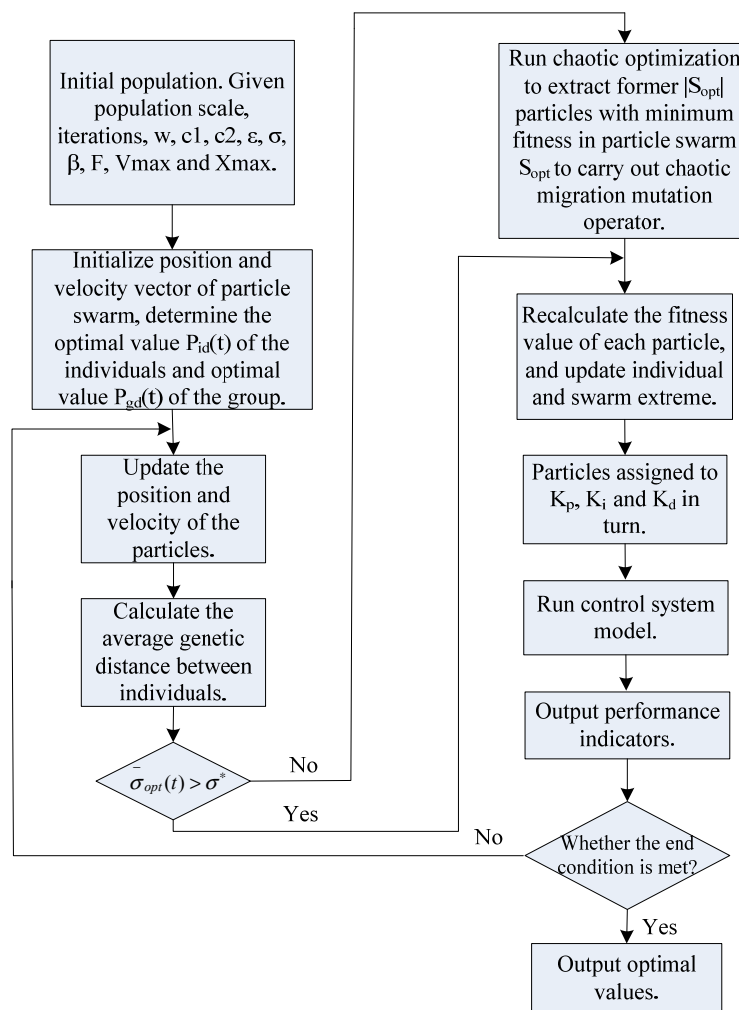
where  $x_{id}^{(1)}(t), x_{id}^{(2)}(t), x_{id}^{(3)}(t)$  are different random individuals in the particle swarm  $S_{opt}$ ,  $\lambda$  is the migration factor,  $F$  is the scale factor,  $t$  is the current iteration and  $T$  is the maximum iteration number.

3.5. Algorithmic Procedure

The flowchart that the proposed hybrid PSO algorithm optimizes the PID controller parameters is shown in Figure 4. The learning steps of the proposed algorithm are states as follows [22].

(1) Initialization population. Initialize the population size, random positions, particle velocities, inertia weights, learning factor, collection valve value, chaos perturbation range  $[-\beta, \beta]$ , scale factor  $F$ , maximum iteration number, the particle’s position range  $[-x_{max}, x_{max}]$  and the particle flight speed range  $[-v_{max}, v_{max}]$ .

Figure 4. Algorithm flowchart.



(2) Calculate the fitness of each particle, and determine the optimal value  $P_{id}(t)$  of each particle and the optimal value  $P_{gd}(t)$  of the whole particle swarm.

(3) According to Equations (19) and (20), the particle’s position and velocity are updated. Then update the individual optimal value  $P_{id}(t)$  of the particle and the optimal values  $P_{gd}(t)$  of particle swarm.

(4) Equations (21)–(23) are utilized to calculate the average distance  $\bar{\sigma}_{opt}(t)$  between particles. Then compare  $\bar{\sigma}_{opt}(t)$  and  $\sigma^*$ . If  $\bar{\sigma}_{opt}(t) > \sigma^*$ , go to step 5. If  $\bar{\sigma}_{opt}(t) \leq \sigma^*$ , judge whether the optimal termination condition is satisfied or not. If it is met, the optimization process is finished and output the optimal results. Otherwise, return to step 2.

(5) According to Equations (24) and (25), the chaotic optimization is processed. Extract the former  $|S_{opt}|$  particle with minimum fitness to take the place of the individuals in the original particle swarm  $S_{opt}$ . According to Equations (26) and (27), the chaotic migration mutation operation is carried out. After the mutation operation, return to step 2.

#### 4. Simulation Experiments

##### 4.1. Input-Output Characteristics of ESR Process

Firstly, the simulation experiments are carried out to observe the control results before decoupling, where two input signals  $X_1$  and  $X_2$  are chosen. The coupling response curves with the input signal  $X_1 = 1$  and  $X_2 = 0$  are shown in Figure 5. The coupling response curves with the input signal  $X_2 = 1$  and  $X_1 = 0$  are shown in Figure 6.

**Figure 5.** System response curves with input signal  $X_1 = 1$  and  $X_2 = 0$ .

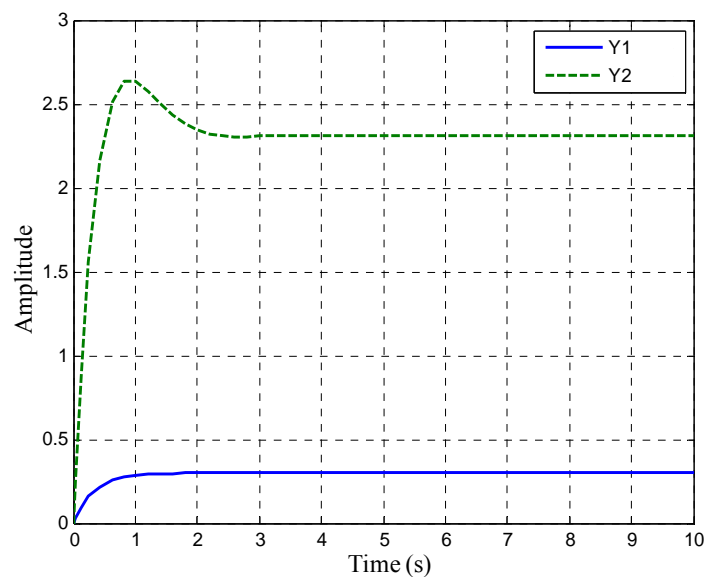
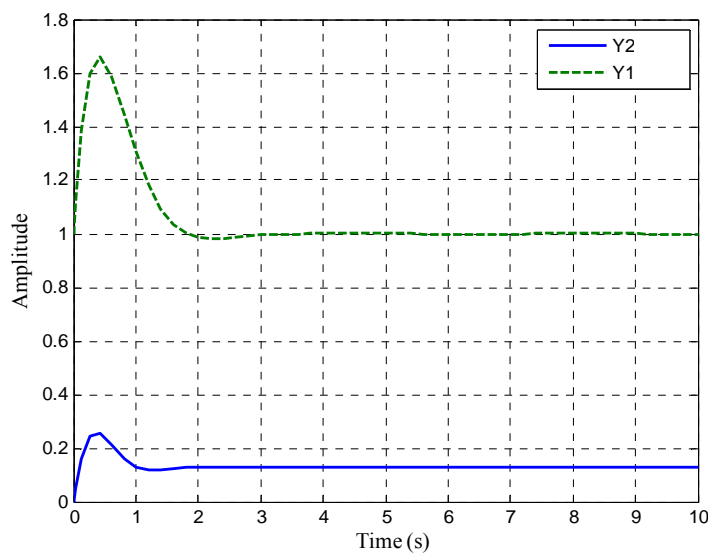


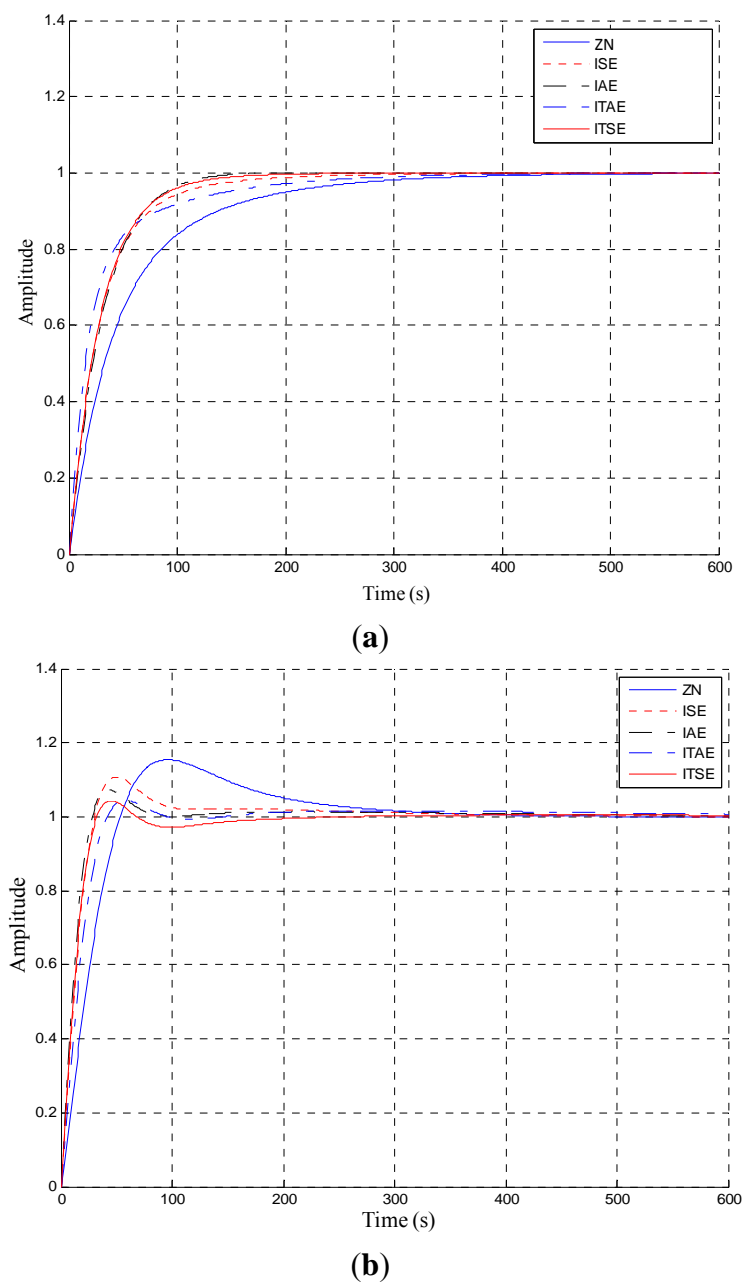
**Figure 6.** System response curves with input signal  $X_1 = 0$  and  $X_2 = 1$ .



4.2. PID Controller Optimized by IPSO Algorithm

This paper utilizes the PID diagonal matrix decoupling controller to control the ESR process. The original coupling control system is divided into two independent control loops. The parameters of the PID controller are optimized by the proposed hybrid particle swarm optimization algorithm on two independent control channels. The paper contrasts the simulation control performances of Z-N method and four different kinds of fitness functions (ISE, IAE, ITAE and ITSE). The simulation results are shown in Figure 7 by adopting the proposed decoupling control strategy on the ESR process.

**Figure 7.** Output responses corresponding to different PID tuning methods. (a) Response curves of output 1; (b) Response curves of output 2.



The optimized PID controller parameters are shown in Table 1. The statistical datum of the system performance (overshoot, rising time and adjusting time) are shown in Table 2. By carrying out the

comparison of simulation results and performance index with the above discussed the equivalent decoupling controlled models in various fitness functions, it can be seen that the control effect under ITAE fitness function is optimal among other fitness functions, which is suitable to realize the decoupling control of the ESR process.

**Table 1.** Tuned parameters of PID controllers.

PID Parameters	System 1					System 2				
	ZN	ISE	IAE	ITAE	ITSE	ZN	ISE	IAE	ITAE	ITSE
$K_p$	4.61	4.94	7.59	8.75	8.59	4.61	7.21	3.20	7.21	7.86
$K_i$	5.90	7.58	9.70	9.70	9.22	5.90	1.63	3.49	8.7	1.26
$K_d$	0.85	0.60	1.61	1.61	1.29	0.85	0.33	0.09	0.09	0.42

**Table 2.** Performance indices of PID controllers.

Performance Indices	System 1					System 2				
	ZN	ISE	IAE	ITAE	ITSE	ZN	ISE	IAE	ITAE	ITSE
Overshoot (%)	0.32	0.25	0.27	0.23	0.43	2.44	2.40	1.93	1.43	1.60
Tr (s)	0.87	0.75	0.64	0.60	0.71	0.94	0.88	0.79	0.60	0.68
Ts (s)	1.24	0.96	1.01	0.81	0.87	4.32	4.01	4.11	3.50	3.97

## 5. Conclusions

Based on the technological characteristics, a PID decoupling control strategy based on the improved particle swarm optimization algorithm is proposed. The simulation results indicated that the proposed control strategy has many characteristics of good dynamic and steady performance, strong robustness and the adaptability of the various working conditions and anti-interference capacity.

## Acknowledgments

This work is partially supported by the Program for China Postdoctoral Science Foundation (Grant No. 20110491510), the Program for Liaoning Excellent Talents in University (Grant No. LJQ2011027), the Program for Anshan Science and Technology Project (Grant No. 2011MS11) and the Program for Research Special Foundation of University of Science and Technology of Liaoning (Grant No. 2011zx10).

## Author Contributions

Jie-Sheng Wang participated in the concept, design, interpretation and commented on the manuscript. A substantial amount of Chen-Xu Ning's contribution to the draft writing and critical revision of this paper was undertaken. Yang Yang participated in the data collection, analysis and algorithm simulation. All authors read and approved the manuscript.

## Conflicts of Interest

The authors declare no conflict of interest.

## References

1. Cao, F.; Wang, W.; Wang, J.-S. Intelligent optimal setting control of electroslag remelting process based on knowledge mining and case-based reasoning. *Inf. Control* **2010**, *39*, 114–119, (in Chinese).
2. Li, B.; Wang, F.; Shan, M. Numerical Analysis of Electromagnetic Field in an Electroslag Remelting Process with Three-Phases Electrodes. In *CFD Modeling and Simulation in Materials Processing*; MNastac, L., Zhang, L., Thomas, B.G., Sabau, A., Ei-Kaddah, N., Powell, A.C., Combeau, H., Eds.; Wiley: Hoboken, NJ, USA, 2012; pp. 131–138.
3. Weber, V.; Jardy, A.; Dussoubs, B.; Ablitzer, D.; Rybéron, S.; Schmitt, V.; Hans, S.; Poisson, H. A comprehensive model of the electroslag remelting process: Description and validation. *Metall. Mater. Trans. B* **2009**, *40*, 271–280.
4. Zhang, L.; Wang, J.-C.; Wang, J.-B. Analysis and application of two principles for ESR furnace swing control. *Metall. Ind. Autom.* **2006**, *2*, 53–55, (in Chinese).
5. Li, W.-Z.; Jia, X.-H.; Wang, J.-C.; Lin, Y.-S. Improvement of consarc ESR furnace control system. *J. Iron Steel Res.* **2007**, *19*, 99–101, (in Chinese).
6. Zhao, L.-L.; Song, J.-C.; Liu, X.-H.; Liu, H.-Y. Intelligent control study based on genetic algorithm for electroslag remelting process. *Mach. Electron.* **2008**, *5*, 16–19, (in Chinese).
7. Ren, W.; Zheng, X.-F.; Jiang, L.-X. Fuzzy adaptive PID control for electrode regulating system of electroslag furnace. *Metall. Ind. Autom.* **2006**, *1*, 15–18, (in Chinese).
8. Jin, Y.C.; Ryu, K.H.; Sung, S.W.; Lee, J.; Lee, I.-B. PID auto-tuning using new model reduction method and explicit PID tuning rule for a fractional order plus time delay model. *J. Process Control* **2014**, *24*, 113–128.
9. Dey, C.; Mudi, R.K. An improved auto-tuning scheme for PID controllers. *ISA Trans.* **2009**, *48*, 396–409.
10. Jin, Q.B.; Hao, F.; Wang, Q. A multivariable IMC-PID method for non-square large time delay systems using NPSO algorithm. *J. Process Control* **2013**, *23*, 649–663.
11. Sarkar, B.K.; Mandal, P.; Saha, R.; Mookherjee, S.; Sanyal, D. GA-optimized feedforward-PID tracking control for a rugged electrohydraulic system design. *ISA Trans.* **2013**, *52*, 853–861.
12. Wang, J.; Wang, J.; Wang, W. Self-tuning of PID parameters based on particle swarm optimization. *Control Decis.* **2005**, *20*, 73–76, (in Chinese).
13. Xiong, W.; Xu, B.; Zhou, Q. Study on optimization of PID parameter based on improved PSO. *Comput. Eng.* **2005**, *31*, 41–43, (in Chinese).
14. Cao, F.; Wang, W. Harmony search based particle swarm optimisation approach for optimal PID control in electroslag remelting process. *Int. J. Model. Identif. Control* **2012**, *15*, 20–27.
15. Wang, D.-Y.; He, G.-Q.; Song, W.-M.; Kang, Y.-J.; Liu, J.-Z. Study and application on intelligent control of the ESR process. *Ind. Heat.* **2005**, *34*, 42–45, (in Chinese).
16. Ahn, S.; Beaman, J.J.; Williamson, R.L.; Melgaard, D.K. Model-Based control of electroslag remelting process using unscented kalman filter. *J. Dyn. Syst. Meas. Control* **2010**, *132*, doi:10.1115/1.4000660.
17. Kennedy, J.; Eberhart, R. Particle Swarm Optimization. In Proceedings of the IEEE International Conference on Neural Networks, Perth, Australia, 27 November–1 December 1995; pp. 760–766.

18. Wang, F.; Yu, P.L.H.; Cheung, D.W. Combining technical trading rules using particle swarm optimization. *Expert Syst. Appl.* **2014**, *41*, 3016–3026.
19. Cheng, S.; Shi, Y.; Qin, Q. A study of normalized population diversity in particle swarm optimization. *Int. J. Swarm Intell. Res.* **2013**, *4*, 1–34.
20. Ren, Z.; San, Z.; Chen, J. Improved particle swarm optimization and its application research in tuning of PID parameters. *J. Syst. Simul.* **2006**, *18*, 2870–2873, (in Chinese).
21. Che, L.; Cheng, Z. Hybrid discrete differential evolution with a self-adaptive penalty function for constrained engineering optimization. *J. Mech. Eng.* **2011**, *47*, 141–151, (in Chinese).
22. Hu, W.; Xu, F. Self-tuning of PID parameters based on improved particle swarm optimization. *Appl. Res. Comput.* **2012**, *29*, 1791–1794, (in Chinese).

© 2014 by the authors; licensee MDPI, Basel, Switzerland. This article is an open access article distributed under the terms and conditions of the Creative Commons Attribution license (<http://creativecommons.org/licenses/by/3.0/>).